

Journal of Materials Chemistry C

Accepted Manuscript



This is an *Accepted Manuscript*, which has been through the RSC Publishing peer review process and has been accepted for publication.

Accepted Manuscripts are published online shortly after acceptance, which is prior to technical editing, formatting and proof reading. This free service from RSC Publishing allows authors to make their results available to the community, in citable form, before publication of the edited article. This *Accepted Manuscript* will be replaced by the edited and formatted *Advance Article* as soon as this is available.

To cite this manuscript please use its permanent Digital Object Identifier (DOI®), which is identical for all formats of publication.

More information about *Accepted Manuscripts* can be found in the [Information for Authors](#).

Please note that technical editing may introduce minor changes to the text and/or graphics contained in the manuscript submitted by the author(s) which may alter content, and that the standard [Terms & Conditions](#) and the [ethical guidelines](#) that apply to the journal are still applicable. In no event shall the RSC be held responsible for any errors or omissions in these *Accepted Manuscript* manuscripts or any consequences arising from the use of any information contained in them.

Cite this: DOI: 10.1039/c0xx00000x

PAPER

www.rsc.org/xxxxxx

Electroluminescent properties of lanthanide pentafluorophenolates

Anatoly P. Pushkarev,^a Vasily A. Ilichev,^a Alexander A. Maleev,^a Anatoly A. Fagin,^a Alexey N. Konev,^a Alexander F. Shestakov,^b Roman V. Rumyantsev,^a Georgy K. Fukin^a and Mikhail N. Bochkarev^{*a}

Received (in XXX, XXX) Xth XXXXXXXXX 20XX, Accepted Xth XXXXXXXXX 20XX

DOI: 10.1039/b000000x

Lanthanide pentafluorophenolates $\text{Ln}(\text{OC}_6\text{F}_5)_3(\text{L})_x$ (Ln = Pr, Nd, Sm, Eu, Dy, Ho, Er, Yb; L = 1,10-phenanthroline, 2,2'-bipyridine; x = 1, 2) are used as emissive layers in organic light emitting devices (OLEDs). Single-layer ITO/ $\text{Ln}(\text{OC}_6\text{F}_5)_3(\text{L})_x/\text{Yb}$ devices reveal no electroluminescence (EL) with the exception of Tb-derivatives-based OLEDs. Bilayer ITO/TPD/ $\text{Ln}(\text{OC}_6\text{F}_5)_3(\text{L})_x/\text{Yb}$ samples exhibit a broad band emission peaked at 580 nm assigned to electroplex at the TPD/complex interface. Besides, the spectra of the devices based on Pr, Nd, Sm, Eu, Er, Tb and Yb derivatives contain the characteristic narrow bands of f-f transitions. Terbium-based bilayer OLEDs exhibit unusual changes in the EL spectra with increasing the applied voltage. The emission color of the devices tunes from orange towards green. The possible nature of the phenomenon is discussed.

1. Introduction

It is known that the luminescence properties of organic complexes of non-transition, d-transition and lanthanide metals in a great extent depend on the nature of the ligands. Analysis of literature data reveals that virtually all of metal-organic luminophores contain bi- or polydentate ligands which provide an extended conjugated chains (necessary for luminescence) and sufficient stability of the material.¹⁻⁵ In the case of organolanthanide emitters the ligands play a role of sensitizers, excitation energy from which is transferred to emissive f sublevels of the metal ion increasing their luminescence.⁶⁻⁸ Fluorescent complexes with monodentate anionic ligands are rare. The group of luminophores containing one monodentate ligand is limited by 8-oxiquinolinolate-aryloxides of aluminum (or gallium) of the type $\text{Al}(\text{q})_2(\text{OR})$,⁹⁻¹⁴ and similar N,N-bis(3,5-di-*tert*-butyl-salicylidene)-ethylenediamine derivatives ($(\text{Bu})_4\text{Al}(\text{OC}_6\text{H}_4\text{-}p\text{-R})$).¹⁵ Photo- or electroexcitation of the complexes results in blue or green-blue emission of moderate efficiency. The luminescent properties of the complexes with two monodentate ligands were not studied. A set of metal-organic luminophores with three non-chelating anionic OC_6F_5 and SC_6F_5 ligands has been prepared and studied by Brennan, Riman and coauthors.¹⁶⁻²⁰ The complexes $(\text{DME})_2\text{Ln}(\text{OC}_6\text{F}_5)_3$ (Ln = Nd, Er, Tm)²⁰ and $(\text{DME})_2\text{Ln}(\text{SC}_6\text{F}_5)_3$ (Ln = Nd¹⁹, Er¹⁷, Tm¹⁸) showed significantly greater metal-centered NIR PL efficiency than that of previously reported non-fluorinated compounds. High quantum yield of metal-centered PL was observed for the clusters containing thiophenolate and selenophenolate ligands $(\text{THF})_8\text{Nd}_8\text{O}_2\text{Se}_2(\text{SePh})_{16}$,¹⁹ $(\text{THF})_6\text{Tm}_4\text{Se}_9(\text{SC}_6\text{F}_5)_2$, $(\text{DME})_4(\mu_2\text{-SPh})_8\text{Tm}_4(\text{SPh})_4$.¹⁸ Both, the absence of C-H bonds in the anionic

ligand and the low Ln-S or Ln-Se phonon energies are thought to minimize competitive vibrational relaxation pathways, and in turn result in the formation of exceptionally emissive molecules. As far as we know, the EL properties of the complexes with exclusively non-chelating anionic ligands have never been studied. To close this gap, we synthesized a series of lanthanide pentafluorophenolates and tested them as emissive materials in single- and bilayer OLED devices.

2. Results and discussions

2.1. Synthesis

Among the lanthanide complexes with pentafluorophenolate ligands the promising as emitters in the OLED devices could be simplest tris(phenolates) $\text{Ln}(\text{OC}_6\text{F}_5)_3$ because they do not contain the ancillary groups with luminescence quenching C-H, N-H or O-H fragments. However, low thermal stability and high hygroscopicity of these compounds²¹ prevent the preparation of thin films by vacuum sublimation or spin-coating methods. In the case of vacuum deposition the complexes explode on the evaporator, while the films prepared from solutions by spin-coating are quickly destroyed because of water absorption. Both these drawbacks of the tris(phenolates) are caused by open coordination sphere of the metal ion (vide infra). To solve the problem we synthesized the phenolates containing 1,10-phenanthroline ($\text{Ln}(\text{OC}_6\text{F}_5)_3(\text{phen}) - \mathbf{1}$ (Ln), $\text{Tb}(\text{OC}_6\text{F}_5)_3(\text{phen})_2 - \mathbf{2}$) or 2,2'-bipyridine ($\text{Tb}(\text{OC}_6\text{F}_5)_3(\text{bpy}) - \mathbf{3}$, $\text{Tb}(\text{OC}_6\text{F}_5)_3(\text{bpy})_2 - \mathbf{4}$) as neutral ancillary ligands. As expected, the introduction of additional groups in the coordination sphere of the lanthanides significantly increased thermal and hygroscopic stability of the complexes.²¹

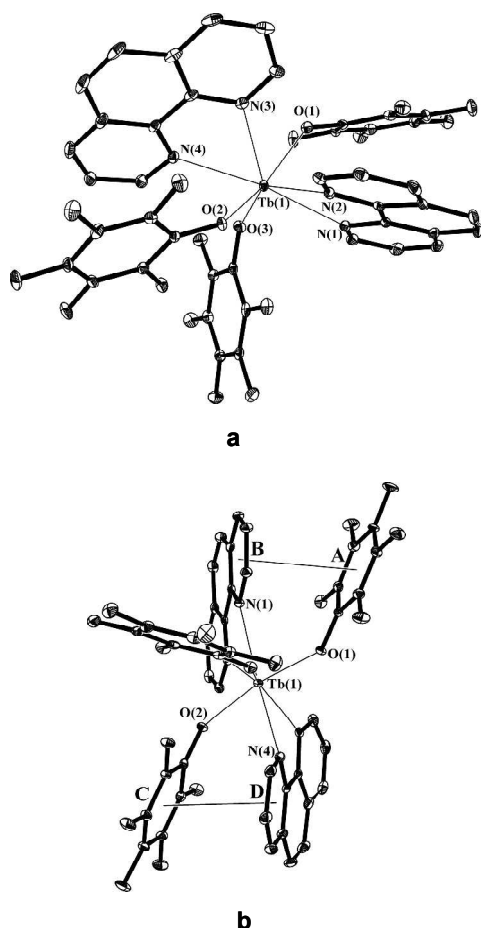


Fig. 1 Molecular structure of $\text{Tb}(\text{OC}_6\text{F}_5)_3(\text{phen})_2$ (**2**). Selected distances [Å] and angles [°]: $\text{Tb}(1)\text{-O}(3)$ 2.1934(17), $\text{Tb}(1)\text{-O}(1)$ 2.2248(17), $\text{Tb}(1)\text{-O}(2)$ 2.2354(16), $\text{Tb}(1)\text{-N}(2)$ 2.5310(19), $\text{Tb}(1)\text{-N}(3)$ 2.542(2), $\text{Tb}(1)\text{-N}(1)$ 2.564(2), $\text{Tb}(1)\text{-N}(4)$ 2.571(2), $\text{N}(2)\text{-Tb}(1)\text{-N}(1)$ 64.30(6), $\text{N}(3)\text{-Tb}(1)\text{-N}(4)$ 64.22(7), $\text{C}(1)\text{-O}(1)\text{-Tb}(1)$ 138.63(16), $\text{C}(7)\text{-O}(2)\text{-Tb}(1)$ 143.55(14), $\text{C}(13)\text{-O}(3)\text{-Tb}(1)$ 143.14(16).

2.2. Structure

According to X-ray analysis the $\text{Tb}(1)$ atom in **2** is bounded by three pentafluorophenolate ligands and two 1,10-phenanthroline molecules (Fig. 1a). In an asymmetric unit there are also two solvate molecules of benzene. Atom $\text{Tb}(1)$ in **2** has a distorted pentagonal-bipyramidal environment. The $\text{Tb}\text{-O}(\text{OC}_6\text{F}_5)$ bond lengths range from 2.1934(17) to 2.2354(16) Å in **2**. Interesting to note that the maximal $\text{Tb}(1)\text{-O}(1, 2)$ distances are observed for pentafluorophenolate ligands disposed in *trans*-position relative to each other (2.2248(17), 2.2354(16) Å). The same situation takes places in related $(\text{THF})_3\text{Yb}(\text{OC}_6\text{F}_5)_3$ and $(\text{THF})_3\text{Ln}(\text{EC}_6\text{F}_5)_3$ ($\text{Ln}=\text{Er}, \text{Yb}; \text{E}=\text{S}, \text{Se}$)^{20,22} complexes containing THF molecules as the neutral ligands. The $\text{Tb}\text{-N}$ distances are 2.5310(19) - 2.571(2) Å. The shortest $\text{Tb}\dots\text{F}$ contact in the molecule is at 3.312(3) Å which excludes possible dative $\text{Tb}\text{-F}$ interaction.

The dihedral angles between pentafluorophenolate and 1,10-phenanthroline ligands (Fig. 1b) are 20.0° (A and B) and 18.8° (C and D). At the same time the distances between the centers of rings A and B, C and D are equal 3.621 and 3.527 Å that satisfy the conditions of intramolecular $\pi\text{-}\pi$ interactions.²³ Besides, relative positions of OC_6F_5 and 1,10-phenanthroline ligands in adjacent molecules in a crystal (centroid-centroid distance is

3.560 Å) indicate an existence of some intermolecular $\pi\text{-}\pi$ interactions.

Our attempts to prepare other phenolates in the crystalline form suitable for X-ray analysis failed. The structures some of the complexes were determined using Quantum chemical modeling. According to these data the complex **1**(Tb) exists in the form of dimer with two $\text{C}_6\text{F}_5\text{O}$ bridges $(\text{phen})\text{Tb}(\text{OC}_6\text{F}_5)_2(\mu\text{-OC}_6\text{F}_5)_2\text{Tb}(\text{OC}_6\text{F}_5)_2(\text{phen})$ (Fig. S1). Energy of this molecule is 19 kcal/mol lower than that of system of two monomers $\text{Tb}(\text{OC}_6\text{F}_5)_3(\text{phen})$ (Fig. S2(a)) and 34 kcal/mol lower than that of the dimer with bridging phen ligands (Fig. S3). The phenolates **1**(Pr, Nd, Sm, Yb) are isostructural to **1**(Tb) (Table S1).

The DFT calculations revealed as well that in three coordinated phenolates $\text{Ln}(\text{OC}_6\text{F}_5)_3$ there are weak intermolecular $\text{F}\rightarrow\text{Ln}$ interactions in axial directions. These interactions persist in dimer form with four $\text{C}_6\text{F}_5\text{O}$ bridges (Fig. S4) which is formed with energy gain ca. 40 kcal/mol. Presumably, such an interaction causes low thermal stability of the perfluorinated phenolates free of ancillary neutral ligands because facilitates the formation of strong $\text{Ln}\text{-F}$ bonds. Coordination to the metal center of 1,10-phenanthroline or 2,2'-bipyridine molecules in mononuclear complexes $\text{Ln}(\text{OC}_6\text{F}_5)_3$ leads to large energy release about 45 and 25 kcal/mol for the first and the second neutral ligand, respectively, and suppresses the dimerization. Since the coordination sphere of the metal ion turned out filled the coordination $\text{F}\rightarrow\text{Ln}$ or $\text{H}_2\text{O}\rightarrow\text{Ln}$ is hindered resulting in enhance the thermal and hygroscopic stability.

2.3. Electroluminescence

The complexes $\text{Ln}(\text{OC}_6\text{F}_5)_3(\text{phen})$, $\text{Ln}(\text{OC}_6\text{F}_5)_3(\text{phen})_2$, $\text{Ln}(\text{OC}_6\text{F}_5)_3(\text{bpy})$, $\text{Ln}(\text{OC}_6\text{F}_5)_3(\text{bpy})_2$ can be sublimed in vacuum or spin casted from solutions to give amorphous stable in air stout entire films. That feature allowed to use them as emissive layers in OLEDs and investigate their EL properties. We have found that the EL properties of all the obtained compounds are similar except the Tb derivatives. In the single-layer devices the tested complexes showed no EL and relatively low charge-transporting properties judging by current-voltage curves (Fig. S8). In contrast, the devices based on Tb-complexes displayed intense bands of $^5\text{D}_4\rightarrow^7\text{F}_j$ ($j=6-3$) transitions characteristic of Tb^{3+} ion (Fig. S9).

It is known that the insertion of the hole-transporting layer (HTL) between the anode and the emissive layer as well as the hole-blocking layer (HBL) between the emissive layer and cathode as a rule significantly increases efficiency of the OLEDs. In the case of the devices based on lanthanide pentafluorophenolates insertion of HTL also leads to improvement their performance but to a different extent depending on the metal. In OLEDs based on **1**(Pr, Nd, Sm, Eu, Dy, Ho, Er, Yb) insertion of TPD layer between ITO and phenolate layer resulted in appearance of broad band peaked at 580 nm (Table 1, Fig. S10), which can be assigned to emission of the electroplex formed at TPD/complex interfaces. This assumption is confirmed by photoluminescence (PL) spectra of double layer **1**(Ln)/TPD and blend samples **1**(Ln):TPD containing the broad band of TPD at about 420 nm and in the cases of Sm, Dy and Tb derivatives the narrow bands of f-f transitions characteristic of the respective Ln^{3+} cation (Fig. S11). The intensity of the band at 580 nm in the EL spectra varies slightly and the maxima remains virtually the same on going from

Table 1 Performance characteristics of the devices of ITO/TPD/Ln-complex/Yb; (L = OC₆F₅)

Complex	V ₀ [V] ^{a)}	λ _{max} [nm]	L _{max} ^{b)} [cd/m ² , *μW/cm ²]	η _c ^{c)} [cd/A]	η _p ^{c)} [lm/W, **mW/W]	EQE ^{c)} [%]
Pr(L) ₃ (phen)	5	580 602	9 (13)	0.09	0.03	0.09
Nd(L) ₃ (phen)	7.5	580 808 900	5 (20) 18* (20)	0.01 -	<0.01 0.06**	0.14
Sm(L) ₃ (phen)	5	566 600 646	40 (12)	0.35	0.1	1.1
Eu(L) ₃ (phen)	10	580 617	<1 (19)	<0.01	<0.01	<0.01
Dy(L) ₃ (phen)	5	580	25 (17.5)	0.26	0.07	0.21
Ho(L) ₃ (phen)	7	580	25 (18.5)	0.3	0.08	0.24
Er(L) ₃ (phen)	6	580	8 (15)	0.07	0.02	0.06
Yb(L) ₃ (phen)	6	580 979	29 (18.5) 90* (18.5)	0.31 -	0.08 0.8**	1.2

^{a)}Voltage at 0.1 mA/cm²; ^{b)}values in parentheses are the voltage at which the luminance was obtained; ^{c)}value at 12 V.

one lanthanide to another. In the EL spectrum of device ITO/TPD/I(Sm)/Yb the band of the electroplex at 580 nm is overlapped with the band of metal-centered emission at 600 nm (⁴G_{5/2}→⁶H_{5/2} transition) and manifests as a shoulder. Unlike the enhanced PL intensity of the similar lanthanide pentafluorophenolates reported by Brennan and coworkers²⁰, the EL of the bilayer OLEDs based on the obtained compounds turned out comparable or even lower than those of devices with most conventional non-fluorinated organo-lanthanide luminophores.⁶⁻⁸ Extremely poor performance characteristics were found for the diode based on **1**(Eu) which exhibited very weak bands at 580 nm and 615 nm (⁵D₀→⁷F₂ transition). In contrast, the device with **1**(Yb) showed high luminescence efficiency. Weak EL activity of Eu complexes and enhanced characteristics of Yb analogs we observed earlier with substituted phenolates²⁴ and naphtholates²⁵ of these metals. It was assumed that great difference in the EL properties of Eu and Yb derivatives is caused by the difference stability of Ln²⁺ ions and energy levels of excited [Ln³⁺]* ions.²⁵ It is possible that the same reasons are responsible for the difference in EL efficiency of Eu and Yb pentafluorophenolates. Insertion of HBL (Bath, 4,7-biphenyl-1,10-phenanthroline, 20 nm) in the ITO/TPD/**1**(Tb)/Yb device between **1**(Tb) and Yb-cathode did not enhance the brightness but a little increased the operating voltage due to the increased resistance of the sample.

2.4. Electroluminescence of devices based on Tb-complexes

Dramatic difference in EL behavior was found for Tb derivatives. First, in contrast to the phenolates of other lanthanides, the compounds **1**(Tb), **2**, **3** and **4** exhibit the intense metal-centered EL not only in the devices containing hole-transporting layer but also in the single-layer OLEDs. Shape of EL spectra of single-layer devices was virtually the same as that of bilayer samples at high voltage while the luminance intensity (50 cd/m²) and other characteristics (current efficiency 1.12 cd/A, power efficiency 0.3 lm/W, EQE 1.8%) were even higher (Fig. S2). Note, that triplet level of the ligand (20408 cm⁻¹, determined from low temperature PL spectra of **1**(Gd)) matches well with the hypersensitive ⁵D₄

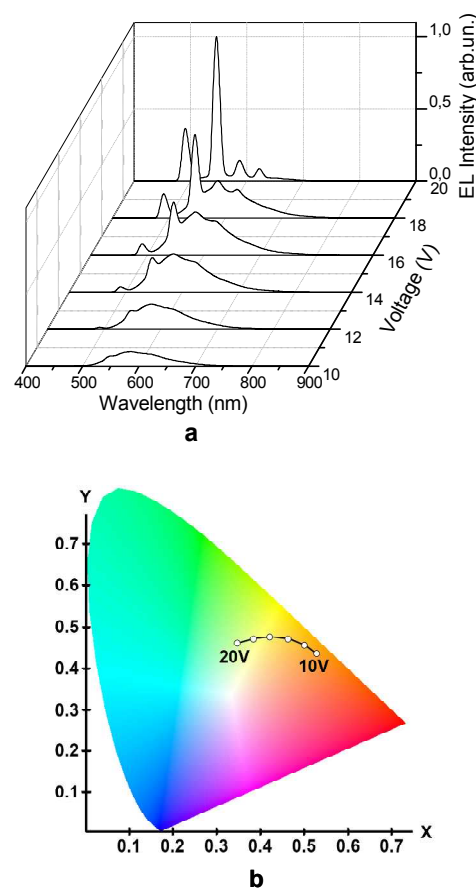


Fig. 2 EL spectra (a) and CIE coordinates (b) of ITO/TPD (20 nm)/**1**(Tb) (40 nm)/Yb device recorded at bias voltage from 10 to 20 V.

level of Tb³⁺ ion (20457 cm⁻¹) providing complete excitation energy transfer from the ligands to the metal. The second, the EL spectra of bilayer devices based on Tb-complexes with TPD or NPD as a HTL vary greatly with voltage increasing. The luminance appeared at 4V as a single broad band centered at 580 nm. Its intensity increased with increasing voltage up to 16 V but then gradually reduced and virtually vanished at 20 V. Simultaneously, at 14 V four characteristic narrow bands arising from Tb³⁺ ion at 491, 546, 586 and 622 nm (⁵D₄→⁷F_j, j=6-3) appeared on a background of the first band. The intensity of these bands run up with voltage increasing and reached maximum at 20 V as it is shown in Fig. 2a for device ITO/TPD/**1**(Tb)/Yb. Change of EL spectra is accompanied by change of the luminance color from orange (CIE, x 0.53; y 0.43) at 10 V to green (CIE, x 0.34; y 0.46) at 20 V (Fig. 2b). The same dependence was found when HTL was N,N'-biphenyl-N,N'-bis(1-naphthyl)-1,1'-biphenyl-4,4'-diamine (NPD) (Table 2). However, the phenomenon was not observed when 4,4'-dicarbazolyl-1,1'-biphenyl (CBP) was used as HTL. The bilayer OLEDs with phenolates of other lanthanides also revealed dependence of EL spectra on applied voltage but to a much lesser degree. No strong enhancement of f-f emission at high voltages was observed but electroplex lumination still tends to decay. Since the ligand composition, structure and energy levels of frontier orbitals, determined from the data of cyclic voltamperometry and DFT calculations (Table S2), are the same or very similar the only explanation for the phenomenon

Table 2 Performance characteristics of the devices of ITO/HTL/Tb-complex/Yb; (L = OC₆F₅)

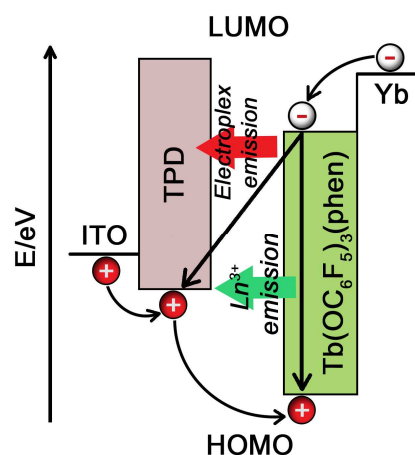
Complex	HTL	Luminance	L _{max} ^{b)} [cd/m ²]	η _c ^{c)} [cd/A]	η _p ^{c)} [lm/W]	EQE ^{c)} [%]
Tb(L) ₃ (phen)	TPD	electroplex f-f	6 (14)	0.31	0.07	0.8
			28.5 (18.5)	0.34	0.06	0.59
			2 (19)	0.05	<0.01	0.13
Tb(L) ₃ (phen) ₂	TPD	electroplex f-f	30 (27)	0.13	0.02	0.25
			31 (23)	0.33	0.05	0.5
			4 (13)	0.35	0.09	0.9
Tb(L) ₃ (bpy)	TPD	electroplex f-f	45 (19)	0.26	0.04	0.45
			1 (13)	0.09	0.02	0.15
Tb(L) ₃ (bpy) ₂	TPD	electroplex f-f	40(19)	0.34	0.05	0.6
			5 (12.5)	0.4	0.1	1.0
			40 (20)	0.35	0.05	0.6

^{a)}Voltage at 0.1 mA/cm²; ^{b)}values in parentheses are the voltage at which the luminance was obtained; ^{c)}value at maximum luminance.

observed in the diodes with terbium complexes is a felicitous correlation energies of the triplet and the resonance levels of Tb³⁺ ion.

The change of EL spectra with increasing of operating voltage is typical for many OLEDs of various compositions.²⁶ However, such dramatic alterations as in the devices with Tb pentafluorophenolates to the best of our knowledge were observed for the first time. In most cases with bilayer and multilayer non-doped devices change of EL spectra upon increasing of applied voltage is explained by the offset of the electron-hole recombination zone from one emissive layers to another due to differences of the energy barriers for the injection of electrons and holes into these layers.²⁷⁻²⁹ In the devices with the doped emissive layers or with blend luminophores the change of voltage-controlled luminance color is caused by shift of the emission from matrix to dopant or from one component of a blend to another.³⁰ The shift of the luminance color from green-yellow to almost white upon increasing the bias voltage in the device based on Pt(acac)(ppy-R) (acac-acetylacetone, ppy-R – substituted phenylpyridyl) complex was explained by the change of the relative triplet-singlet intensity ratio.^{31,32} The dependence of EL spectra on bias voltage for the device with Sm(TTA)₃(TPPO)₂ emissive layer (TTA – thenoyltrifluoroacetone, TPPO – triphenylphosphine oxide) Reyes and coworkers explained by different intensity of the metal-centered and ligand-centered emission at different voltages.³³ The change of visible EL spectra of bilayer device TPD/Ho(DBM)₃(Bath) (DBM – dibenzoylmethanato, Bath – bathophenanthroline) at various voltages the authors attributed to luminescence of interfacial exciplex.³⁴ The emission intensity of the exciplex showed a tendency to saturation at high driving voltage, while the emissions of the Ho³⁺ ions kept increasing resulting in change of the luminance color. Varying of emission colour of bilayer device NPD/Zn(4-TfmBTZ)₂ (4-TfmBTZ – 2-(4-trifluoromethyl-2-hydroxyphenyl)benzothiazole) the authors explained by electroplex formation in the interface.³⁵ The intensity of the electroplex emission was found to decrease progressively with applied voltage.

We suppose that peculiarity of EL of devices based on Tb pentafluorophenolates is also caused by the formation of electroplex at TPD/Tb-complex interface and relatively low hole-

**Chart 1** Scheme of electroplex formation in the TPD/complex interface.

transporting properties of the complexes (Chart 1). At low voltage the holes are not injected into Tb-complex layer but electrons easy pass through it reaching the organic interface and providing the electron-hole recombination at the interfacial area. As indicated above, the emission from the electroplex is observed as a broad band at 580 nm. As the bias increases, the holes begin to inject into the Tb-complex layer and as a result the recombination zone shifts to this layer leading to decrease of the electroplex emission and the appearance of emission of Tb³⁺ cations. In favor of such assumption says absence of a band at 580 nm in the spectra of single-layer devices. Substitution of TPD in the device ITO/TPD/1Tb/Yb with NPD resulted in a decrease of dependence of EL spectrum on voltage. When CBP was used as HTL the phenomenon was not observed at all although intensity of the metal-centered emission remained high in both cases (Table 1). The reason of the difference in luminescence behavior of the devices with TPD (NPD) and CBP layers probably is due to difference in the energy levels of frontier orbitals of these materials (TPD (NPD): HOMO 5.5 eV, LUMO 2.4 eV; CBP: 6.1 and 2.7 eV, respectively³⁶). Change of the number of neutral ligands (compounds 1(Tb)/2; 3/4) and the type of these ligands (complexes 1(Tb)/3; 2/4) does not affect essentially on the EL properties of the OLEDs. These data suggest that the formation of electroplex is the result of a donor-acceptor interaction of the HTL molecules and OC₆F₅ groups but not the phen or bpy ligands in the lanthanide complexes.

3. Experimental Section

3.1. General procedure

The syntheses and manipulations of the compounds described below were realized with exclusion of air and water using Schlenk techniques. Reagent-grade chemicals were used in all experiments, and solvents were purified using standard procedures and collected in a reaction vessel by condensation in vacuum. Pentafluorophenole, 2,2'-bipyridine and 1,10-phenanthroline (purchased from Aldrich) were purified and dried by sublimation under reduced pressure. Silylamides Ln[N(SiMe₃)₂]₃ were prepared according to the published procedures.³⁷ Content of metal in the products was determined by complexometric titration. The lanthanide pentafluorophenolates Ln(OC₆F₅)₃(phen) (1(Pr, Nd, Er)), Tb(OC₆F₅)₃(phen)₂ (2),

Tb(OC₆F₅)₃(bpy)₂ (**4**) were synthesized by the reactions of amides Ln[N(SiMe₃)₂]₃ with pentafluorophenol in benzene or toluene in the presence of 1,10-phenanthroline or 2,2'-bipyridine as described in the paper.²¹ Preparation and characterisation of Ln(OC₆F₅)₃(phen) (**1**(Sm, Eu, Dy, Ho, Tm, Yb)) and Tb(OC₆F₅)₃(bpy) (**3**) are described in the Supplementary information.

3.2. Photophysical measurements

IR spectra were recorded on a Specord M-75 spectrometer from 4000 to 450 cm⁻¹. The samples were prepared as Nujol mulls and as films between KBr plates. UV-vis spectra were recorded with a Perkin Elmer Lambda 25 spectrometer in a region from 200 to 1100 nm. The photoluminescence spectra were recorded from 400 to 800 nm on a spectrometer Perkin Elmer Fluorescence LS-55 (spectral resolution 1 nm) with excitation at 270 nm. The samples were prepared as the films on optical quartz.

3.3. Cyclic voltammetry

Cyclic voltammetry of the complexes was performed in a typical three-electrode cell with a platinum sheet working electrode, a platinum sheet counter electrode (bigger surface), and a silver/silver nitrate (Ag/Ag⁺) pseudoreference electrode.³⁸ All electrochemical experiments were carried out under an argon atmosphere at room temperature in an electrolyte solution of 0.2 M tetrabutylammonium tetrafluoroborate in THF at a sweep rate of 100 mV×s⁻¹. Concentration of investigated compounds was 0.01 M.

3.4. X-ray Crystallography

The X-ray data of **2** was collected on an Agilent Xcalibur E diffractometer (graphite-monochromator, MoK α -radiation, ω -scan technique, $\lambda = 0.71073 \text{ \AA}$, $T = 100(2) \text{ K}$). *ABSPACK (CrysAlis Pro)*³⁹ was used to perform area-detector scaling and absorption corrections. Data Collection, Reduction and Correction Program, CrysAlis Pro – Software Package, Agilent Technologies (2012)⁴⁰ were used to integration of experimental data. The structure was solved by direct methods and was refined on F^2 using *SHELXTL*⁴¹ package. All hydrogen atoms were placed in calculated positions and were refined in the riding model.

The crystal data for **2** (C₅₄H₂₈F₁₅N₄O₃Tb): monoclinic crystal system, space group C2/c, unit cell dimensions $a = 23.7548(2) \text{ \AA}$, $b = 13.8996(1) \text{ \AA}$, $c = 28.8695(2) \text{ \AA}$, $\beta = 100.8412(8)^\circ$, $V = 9362.06(13) \text{ \AA}^3$, $Z = 8$, $d_{\text{calc.}} = 1.738 \text{ g/cm}^3$, $\mu = 1.622 \text{ mm}^{-1}$, $F(000) = 4832$, $R1 = 0.0309$ ($I > 2\sigma(I)$), $wR2 = 0.0636$ (all data), $S(F^2) = 1.147$, largest diff. peak and hole 2.035 and -1.502 e⁻ \AA^{-3} .

CCDC 947374 (**2**) contains the supplementary crystallographic data for this paper. These data can be obtained free of charge via www.ccdc.cam.ac.uk/conts/retrieving.html (or from the Cambridge Crystallographic Data Centre, 12 Union Road, Cambridge CB21EZ, UK; fax: (+44) 1223-336-033; or deposit@ccdc.cam.ac.uk).

3.5. Device fabrication and measurements

The simple single-layer devices ITO/complex(50 nm)/Yb(150 nm), containing complexes **1**(Ln), **2**, **3** and **4** as an emissive layer, were fabricated in a vacuum chamber (10⁻⁶ mbar) with different

resistive heaters for organic and metal layers.⁴² The bilayer devices ITO/HTL(20 nm)/complex(40 nm)/Yb(150 nm) (HTL = TPD, NPD, CBP) were prepared similarly. A commercial ITO on a glass substrate with 5 Ω/\square was used as the anode material (Luminescence Technology Corp.) and commercial Yb, 99.9% trace metals basis (Sigma-Aldrich) as the cathode material. The deposition rate for the TPD and metallo-complexes was 1 nm/s. The active area of the devices was 4×4 mm. The EL spectra in visible region and current-voltage-luminance characteristics were measured with Ocean Optics USB2000 fluorimeter calibrated with Ocean Optics LS-1 CAL lamp, the computer controlled GW Instek PPE-3323 power supply and GW Instek GDM-8246 digital multimeter. The spectra and power efficiency in the NIR region was determined by Ocean Optics NIR-512 spectrometer. The device characteristics measurements were carried out under ambient conditions.

4. Conclusions

The EL properties of lanthanide pentafluorophenolates were studied for the first time. In the single-layer devices the complexes revealed no EL but insertion of HTL resulted in appearance of the metal-centered emission in the cases of Pr, Nd, Sm, Eu and Yb complexes along with the luminescence of electroplex formed at HTL/complex interface which is observed also for the OLEDs based on the Ho and Dy complexes. Efficiency of the metal-centered luminescence is comparable with that of the devices based on conventional non-fluorinated organo-lanthanide luminophores unlike the enhanced PL of perfluorinated lanthanide phenolates. Unusually strong change in the EL spectra and luminance color with increasing the applied voltage was found for the bilayer devices based on Tb-complexes. The observed phenomenon is explained by shifting of recombination zone and respectively the emission from the interfacial HTL/complex electroplex to the layer of Tb-compound that causes metal-centered luminescence. Due to these features, the systems may be used for the fabrication of voltage-color tunable organic LEDs. Besides, the observed tendency of lanthanide pentafluorophenolates to form electroplex with donor compounds suggests that these complexes may be suitable acceptor materials in design of efficient molecular photovoltaic cells. Further investigations in this direction are in progress.

Acknowledgements

This work was partially supported by the Russian Foundation for Basic Research (Grants No. 13-03-00097, 13-03-00891, 12-03-31273, 12-03-31474, 13-03-97046, 13-03-00891) and the Ministry of Education and Science of the Russian Federation (agreement 8637). The authors thank I. D. Grishin for voltammetric measurements.

Notes and references

- ^a G. A. Razuvaev Institute of Organometallic Chemistry of Russian Academy of Sciences, Tropinina 49, 603950 Nizhny Novgorod, Russian Federation. Fax: +7 (831) 4627497; Tel: +7 (831) 4627709; E-mail: mboch@iomc.ras.ru
- ^b Institute of Problems of Chemical Physics of Russian Academy of Sciences, Academician Semenov avenue 1, 142432 Chernogolovka, Russian Federation. Fax: +7(49652) 23507; Tel: +7(49652) 2-44-76

† Electronic Supplementary Information (ESI) available: I-L-V characteristics of devices, EL, PL spectra, HOMO, LUMO values, details of DFT calculations. See DOI: 10.1039/b000000x/

- 5 1 H. Yersin, *Top Carr. Chem.*, 2004, **241**, 1.
2 L. Xiao, Z. Chen, B. Qu, J. Luo, S. Kong, Q. Gong and J. Kido, *Adv. Mater.*, 2011, **23**, 926.
3 H. Sasabe and J. Kido, *Chem. Mater.*, 2011, **23**, 621.
4 K. Walzer, B. Maennig, M. Pfeiffer and K. Leo, *Chem. Rev.*, 2007, **107**, 1233.
10 5 M. N. Bochkarev, A. G. Vitukhnovsky and M. A. Katkova, *Organic Light-emitting Diodes (OLED)*, (Russ.), Dekom, Nizhny Novgorod, Russian Federation, 2011.
6 J.-C. G. Bünzli, *Chem. Rev.*, 2010, **110**, 2729.
15 7 K. Binnemans, *Chem. Rev.*, 2009, **109**, 4283.
8 M. A. Katkova and M. N. Bochkarev, *Dalton Trans.*, 2010, **39**, 6599.
9 J. C. Deaton, D. W. Place, C. T. Brown, M. Rajeswaran and M. E. Kondakova, *Inorg. Chim. Acta*, 2008, **361**, 1020.
20 10 C. Pérez-Bolivar, V. A. Montes and P. Anzenbacher, Jr., *Inorg. Chem.*, 2006, **45**, 9610.
11 M. La Deda, I. Aiello, A. Grisolia, M. Ghedini, M. Amati and F. Leij, *Dalton Trans.*, 2006, 330.
12 G. Giro, M. Cocchi, P. Di Marco, V. Fattori, P. Dembech and S. Rizzoli, *Synth. Met.*, 2001, **123**, 529.
25 13 Z. Shen, P. E. Burrows, V. Bulovic, S. R. Forrest and M. E. Thompson, *Science*, 1997, **276**, 2009.
14 Y. Qiu, Y. Shao, D. Zhang and X. Hong, *Jpn. J. Appl. Phys.*, 2000, **39**, 1151.
30 15 K. Y. Hwang, M. H. Lee, H. Jang, Y. Sung, J. S. Lee, S. H. Kimb and Y. Do, *Dalton Trans.*, 2008, **14**, 1818.
16 J. H. Melman, T. J. Emge and J. G. Brennan, *Inorg. Chem.*, 2001, **40**, 1078.
17 G. A. Kumar, R. E. Riman, L. A. Diaz Torres, O. B. Garcia, S. Banerjee, A. Kornienko and J. G. Brennan, *Chem. Mater.*, 2005, **17**, 5130.
35 18 S. Banerjee, G. A. Kumar, T. J. Emge, R. E. Riman and J. G. Brennan, *Chem. Mater.*, 2008, **20**, 4367.
19 S. Banerjee, L. Huebner, M. D. Romanelli, G. A. Kumar, R. E. Riman, T. J. Emge and J. G. Brennan, *J. Am. Chem. Soc.*, 2005, **127**, 15900.
40 20 K. Norton, G. A. Kumar, J. L. Dilks, T. J. Emge, R. E. Riman, M. G. Brik and J. G. Brennan, *Inorg. Chem.*, 2009, **48**, 3573.
21 A. A. Maleev, A. A. Fagin, V. A. Ilichev, M. A. Lopatin, A. N. Konev, M. A. Samsonov, G. K. Fukin and M. N. Bochkarev, *J. Organomet. Chem.*, DOI.org/10.1016/j.jorganchem.2013.03.052.
45 22 K. Krogh-Jespersen, M. D. Romanelli, J. H. Melman, T. J. Emge and J. G. Brennan, *Inorg. Chem.*, 2010, **49**, 552.
23 C. Janiak, *J. Chem. Soc., Dalton Trans.*, 2000, 3885.
50 24 M. A. Katkova, A. P. Pushkarev, T. V. Balashova, A. N. Konev, G. K. Fukin, S. Yu. Ketkov and M. N. Bochkarev, *J. Mater. Chem.*, 2011, **21**, 16611.
25 A. P. Pushkarev, V. A. Ilichev, T. V. Balashova, D. L. Vorozhtsov, M. E. Burin, D. M. Kuzyaev, G. K. Fukin, B. A. Andreev, D. I. Kryzhkov, A. N. Yablonskiy and M. N. Bochkarev, *Russ. Chem. Bull.* 2013, 395.
55 26 J. Kalinowski, *Organic Light-Emitting Diodes. Principles, Characteristics, and Processes*, Marcel Dekker, New York, USA, 2005.
60 27 J. Kalinowski, P. Di Marco, V. Fattori, L. Giulietti and M. Cocchi, *J. Appl. Phys.*, 1998, **83**, 4242.
28 Y. Z. Wang, R. G. Sun, F. Mehdadi, G. Leising and A. Epstein, *Appl. Phys. Lett.*, 1999, **74**, 3613.
29 R. C. Kwong, S. Sibley, T. Dubovoy, M. Baldo, S. R. Forrest and M. E. Thompson, *Chem. Mater.*, 1999, **11**, 3709.
65 30 J. Kalinowski, M. Cocchi, G. Giro, V. Fattori and P. Di Marco, *J. Phys. D: Appl. Phys.*, 2001, **34**, 2282.
31 Z. He, W.-Y. Wong, X. Yu, H.-S. Kwok and Z. Lin, *Inorg. Chem.*, 2006, **45**, 10922.
70 32 B. W. D'Andrade, J. Brooks, V. Adamovich, M. E. Thompson and S. R. Forrest, *Adv. Mater.*, 2002, **14**, 1032.
33 R. Reyes, M. Cremona, E. E. S. Teotonio, H. F. Brito and O. L. Malta, *J. Lumin.*, 2013, **134**, 369.
34 F. X. Zang, W. L. Li, Z. R. Hong, H. Z. Wei, M. T. Li, X. Y. Sun and C. S. Lee, *Appl. Phys. Lett.*, 2004, **84**, 5115.
75 35 Y. Zhang, Y. Hao, W. Meng, H. Xu, H. Wang and B. Xu, *Appl. Phys. A*, 2012, **106**, 709.
36 K. Müllen and U. Scherf, *Organic Light Emitting Devices: Synthesis, Properties and Applications*, WILEY-VCH, Weinheim, Germany, 2006.
80 37 D. C. Bradley, J. S. Ghotra and F. A. Hart, *J. Chem. Soc., Dalton Trans.*, 1973, 1021.
38 M. A. Vorotyntsev, M. Casalta, E. Pousson, L. Roullier, G. Boni and C. Moise, *Electrochim. Acta*, 2001, **46**, 4017.
85 39 SCALE3 ABSPACK, *CrysAlisPro*, Agilent Technologies (2012).
40 Data Collection, Reduction and Correction Program, *CrysAlisPro – Software Package*, Agilent Technologies (2012).
41 G. M. Sheldrick, *SHELXTL v. 6.12*, Structure Determination Software Suite, Bruker AXS, Madison, Wisconsin, USA, 2000.
90 42 M. N. Bochkarev, M. A. Katkova, V. A. Ilichev and A. N. Konev, *Nanotechnol. Russia*, 2008, **3**, 470.